A.M. WITTEK*, R. BURDZIK**,#, P. FOLĘGA**, Ł. KONIECZNY**, B. ŁAZARZ**

INFLUENCE OF PRODUCTION PROCESS AND MATERIAL FACTORS ON FATIGUE STRENGTH OF TUBULAR STABILIZER BAR

WPŁYW PROCESU PRODUKCYJNEGO I CZYNNIKÓW MATERIAŁOWYCH NA WYTRZYMAŁOŚĆ ZMĘCZENIOWĄ STABILIZATORA RUROWEGO

The paper presented results of the research on process of production of highly important element of passenger car. The main object of the research was influence of production process and material factors on fatigue strength of tubular stabilizer bar. The scope of the research included the stabilizer bar hot bent at the bending table, hardened in oil and tempered. The bending radii I, II and III were metalographically tested. The stabilizer bar was also subjected to fatigue tests. For analysis purpose the finite element method (FEM) calculation have been conducted. The analysis of relationship of outer diameter to wall thickness is very important. The analysed bar has broken early. The paper presents the reasons for premature failure of the tubular stabilizer bar.

Keywords: stabilizer bar, FEM, metalographically test, TTT diagram, equivalent stresses

W artykule przedstawiono wyniki badań procesu produkcji bardzo ważnego elementu zawieszenia pojazdu samochodowego. Głównym celem badań była analiza wpływu czynników procesu produkcyjnego i paramtetrów materiałowych na wytrzymałość zmęczeniową stabilizatora rurowego. Zakres badań obejmował gięty na gorąco stabilizator rurowy, hartowany w oleju i odpuszczany. Promienie gięcia I, II i III zostały poddane testom metalograficznym. Stabilizator poddano również testom zmęczeniowym. Dla celów analizy przeprowadzono obliczenia zmęczeniowe z wykorzystaniem MES. Niezwykle ważna jest analiza stosunku średnicy zewnętrznej do grubości ścianki. Badany stabilizator uległ przedwczesnemu zniszczeniu. W artykule przedstawiono przyczyny przedwczesnego uszkodzenia badanego stabilizatora rurowego.

1. Introduction

The function of stabilizer bars in motor vehicles is to reduce the body roll during cornering. The body roll is influenced by the occurring wheel load shift and the change of camber angle. Decisive is the steering performance which may be purposefully adjusted towards understeer or oversteer when designing the stabilization. The designer has to consider many factors when constructing stabilizer bars. This is of fundamental importance for successful construction and series production as well as for the quality and fatigue strength of the stabilizer bar. Stresses and deformations occurring in the stabilizer bar under load may be calculated using two different methods: analytical calculation and finite element method (FEM). If we consider the loads of stabilizer bars over the material cross–section, we immediately realise that the inner sections are not loaded, so they do not contribute to the function. Therefore, in order to reduce the weight, the tubular stabilizer bars were developed. The relationship of solid bar diameter, tube dimensions, weight saving and stress increase

for a solid bar diameter of 25 mm, as shown in example Fig. 1 [1–6, 9]. Realistically, the weight saving does not exceed 45 % because otherwise the tubes become too thin–walled, and considerable manufacturing difficulties occur. The load also linearly increases with the diameter so that already for this reason natural boundaries are set. That is why a relationship of outer diameter to wall thickness of 6,5 to 7,5 should not be exceeded. In addition, provided that the stabilisation is equal, approx. 6,5 % bigger outer diameters and as a consequence accordingly bigger stresses with a weight saving of approx. 40 % compared to solid bars arise. The points of force transmission in tubular stabilizer bars may be made identically to those of bars of solid material [1–6, 9]. During driving for each vehicle many factors can be determined, like acting mechanical forces, vibration, noises and in consequence determination of the degree of wear, friction and corrosion processes For proper analysis of those phenomenons has to be conducted inter alia, the strength testing and metallographic research. The material properties and metallurgical processes are very important, especially for vehicle elements which correspond

* THYSSENKRUPP FEDERN & STABILISATOREN GMBH, WIENERSTR. 35, 58135 HAGEN, GERMANY

** THE SILESIAN UNIVERSITY OF TECHNOLOGY, FACULTY OF TRANSPORT, KRASIŃSKIEGO 8, 40-019 KATOWICE, POLAND

Corresponding author: rafal.burdzik@polsl.pl

to for safety of driving. There are many new research, reports and papers about novel materials in terms of the properties and metallurgical processes.
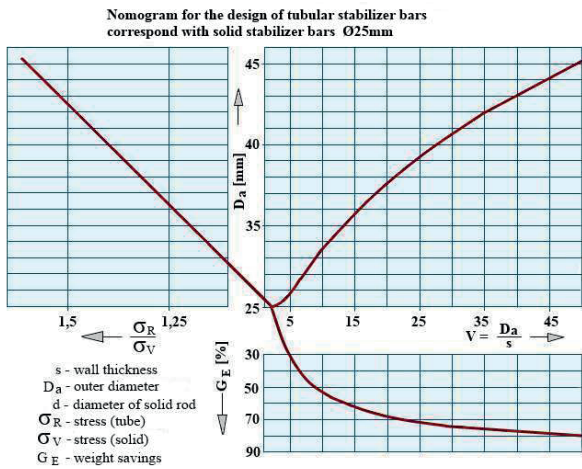

Fig.1. Nomogram for the design of tubular stabilizer bars correspond with solid stabilizer bars Ø25 mm [1–6, 9]

2. Experimental materials and conditions

The stabilizer bar was hot bent at the bending table, hardened in oil and tempered (Table 1). The bending radii I, II and III (Fig. 2) were metalographically tested. The stabilizer bar was also subjected to fatigue tests. For analysis purpose the finite element method [7-9] calculation have been conducted. The stabilizer bar has broken early (it has not reached the specified figures of the load cycles). The reason of it is proeutectoid ferrite precipitations connected with the high load in the bending radii areas.
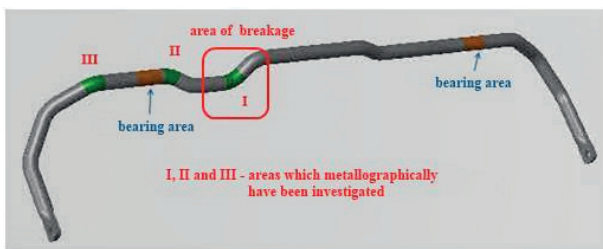

Fig. 2. Tubular stabilizer bar – endangered areas, area of breakage

The metallographic examination of fatigue fractures radial zones of stabilizer bar were carried out in the laboratory of ThyssenKrupp Bilstein Suspension GmbH (Fig. 3) using a Leitz microscope metallographic type Aristomet, coupled with Sony Videoprinter video equipment, cameras Leicaflex, foto–makroskop Wild 400 and a device for measuring surface roughness Perthometer S5P.

TABLE 1

Production parameters

Production parameter	value
tubular stabilizer bar	Ø23,5x3,6 mm

bending radius	50 mm
steel grade	34MnB5, R_m=1700 MPa
forces which act on the ends of stabilizer bar	3575,7 N
spring deflection 2s	86,0mm
stabilizer bar rate	41,6 N/mm
bearings distance	616 mm ±2
leg distance	1024,1 mm ±2
equivalent stress max. (St3d)	890 MPa
bending time	6 sek.
time of bending cycle (until to hardening)	12 sek.
temperature after the conductive heating	940 °C
temperature of stabilizer bar before hardening	856 °C

Fig. 3. Metallographic laboratory of ThyssenKrupp Bilstein Suspension GmbH (source TKBiS)

The fatigue tests were performed on eccentric machine for dynamic tests of stabilizer bars (Fig. 4). The number of fatigue cycles obtained during tests (Fig. 5) (until the destruction of stabilizer) was compared with the results of FEM calculation (using of dynamic fatigue calculation software DesignLife nCode HBM) (Fig. 15).
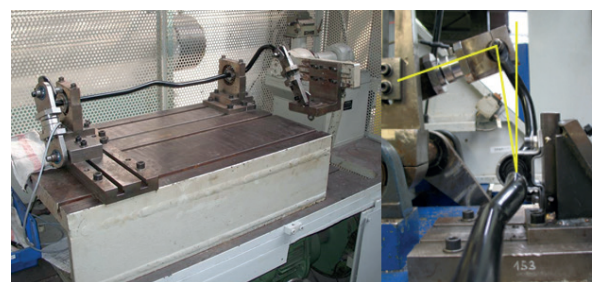

Fig. 4. Eccentric machine for dynamic tests of stabilizer bars (source TKBiS): max. dimensions of stabilizer bar: 1100 x 350 mm, diameter of stabilizer bar: 10 – 25 mm, max. forces acting on the ends of the stabilizer bar: ± 4 kN, angle of oscillation: ± 40°, frequency: 0,5 – 4 Hz

The FEM strength calculations (static calculations – Fig. 13, 14 and dynamic calculations – Fig. 15) were carried out using programs HyperWorks + Radioss (Altair) and nCode DesignLife (HBM).

On microscopic evaluation, the depth of decarburization is based on structural changes determined (according to DIN EN ISO 3887) [10]. At ferrite–pearlite structures in the decarburization edge zone a can be observed with higher ferrite content. If there is a soft annealing structure, the

decarburization shall be determined by a reduction of the carbide content in the ferritic matrix.
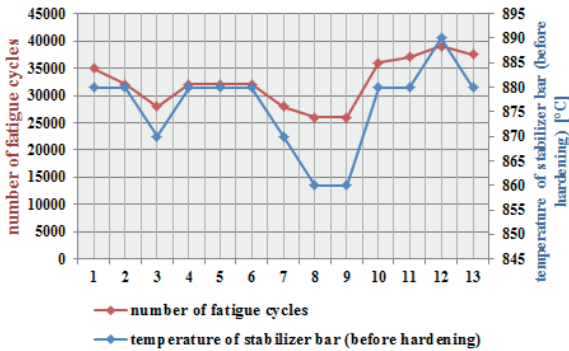

Fig. 5. The results of fatigue tests carried out on the machine shown in Fig. 4

3. Results

Solid stabilizer bars are manufactured of heat–treated steels according to DIN 17200 and 17221. For tubular stabilizer bars primarily micro–alloyed steels such as 26MnB5 and 34MnB5 (Table 2), which may be either hot or cold bent, are used. The maximum allowable strength, thus the load is determined in the first approximation by the carbon content. In case of welded tubes the maximum carbon content is limited by the welding process. If the carbon content of an alloy is not sufficient in order to set a desired strength, the stabilizer bar manufacture must be preceded by a carbonisation process of the semi–finished tube (Fig. 6).

TABLE 2

Chemical composition 34MnB5 [14]

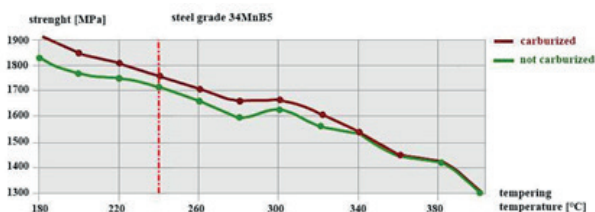| type of steel	number of steel	C	Si	Mn	P
34MnB5	11.166	0,338	0,24	1,22	0,01
		S	Al	N	Nb
		0,001	0,03	0,0044	0,001
		V	Mo	B	Cu
		0	0,01	0,0021	0,01
		Cr	Ni	Ti	
		0,13	0,02	0,03	

Fig. 6. Tempering curves of the steel grade 34MnB5 [5]

Ferrite is a solid, interstitial carbon solution in iron which forms through entering of carbon atoms into octahedral voids, which are flattened, and into tetrahedral voids (Fig. 7). The fact that the carbon atom diameter is greater than the diameter of the voids causes that the solubility of carbon is low and does not exceed 0,022%. Ferrite as a separate structural constituent occurs in hypoeutectoid steels so called proeutectoid ferrite. In view of a low carbon content the properties of ferrite do not differ much from the properties of pure iron α so that R_m = about 300 MPa, 80 HB, A_{10} = 40%, KC = about 180 J/cm^2. It is visible as a bright constituent in the metallographic specimens.

TABLE 3

Production parameters

example / radius		decarburization	forming of steel microstructure		drawing
I	outside of tube	the sample is over the entire cross–section: martensite and formation - excretion of proeutectoid ferrite 0,18 mm			drawing 7 a ÷ e
	inside of tube				
II	outside of tube	formation - excretion of proeutectoid ferrite 0,13 mm		martensite + proeutectoid ferrite	drawing 8 a ÷ c
	inside of tube	decarburization: ca. 0,01mm formation - excretion of proeutectoid ferrite 0,13 mm			
III	outside of tube	formation - excretion of proeutectoid ferrite 0,14 mm		martensite	drawing 9 a ÷ b
	inside of tube	decarburization: ca. 0,01mm formation - excretion of proeutectoid ferrite 0,08 mm			

Proeutectoid ferrite occurs in the form of separate grains alternately with the pearlite grains (cellular structure) or at the boundaries of the pearlite grains [15]. The stabilizer bar shows the highest percentage of ferrite in the back (bending radius I). It tends to decrease towards the arms (radii II and III – Figures 8 and 9), according to the bending sequence. The percentage of ferrite, however, is generally too high. The values in the amount of 0,15 mm will not lead (Table 3) to the fatigue fracture. The values above 0,15 mm lead to the fatigue fracture and thus premature failure of the stabilizer bar.
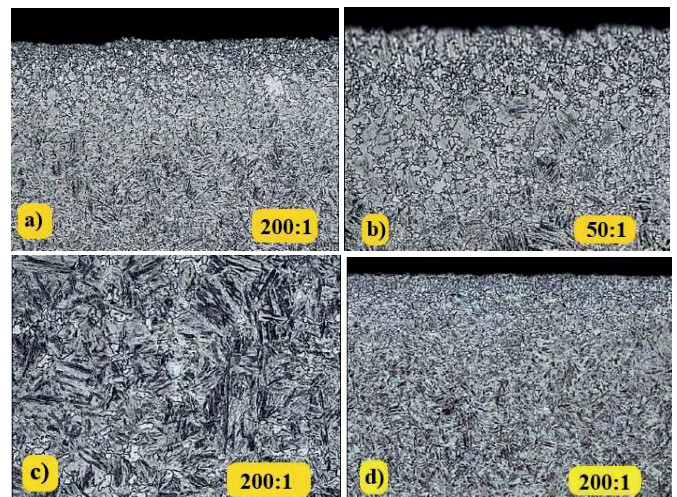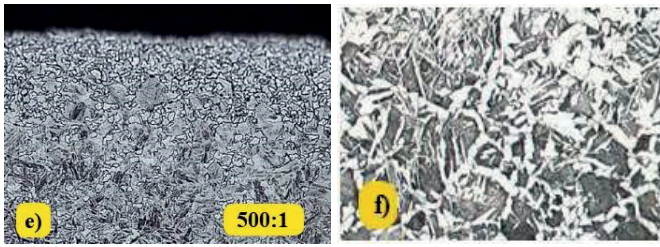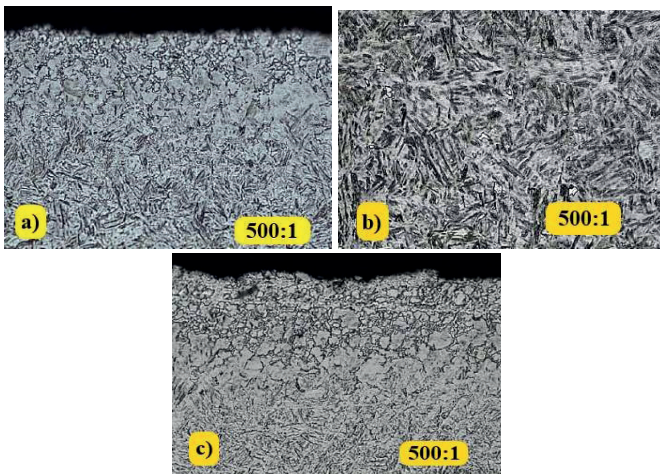
Fig. 7. The microstructure formation – inside and outside of the tube (cross section I) [11, 12, 13]:
a) radius I / inside bending radius, tube outside, etched with 1% HNO₃, 200:1,
b) radius I / inside bending radius, tube outside, etched with 1% HNO₃, 50:1,
c) radius I / core, etched with 1% HNO3, 200:1,
d) radius I / inside bending radius, tube inside, etched with 1% HNO3, 200:1,
e) radius I / inside bending radius, tube inside, etched with 1% HNO₃, 500:1,
f) precipitates of proeutectoid ferrite

Fig. 8. The microstructure formation – inside and outside of the tube (cross section II) [11, 12, 13]:
a) radius II / inside bending radius, tube outside, etched with 1% HNO₃, 500:1,
b) radius II / core, etched with 1% HNO₃, 500:1,
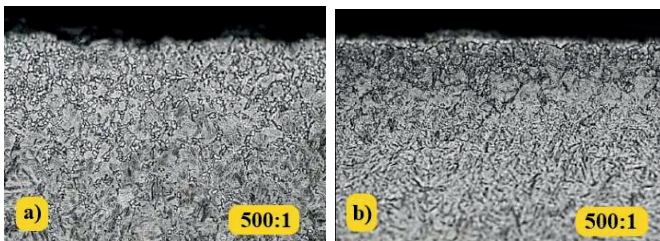c) radius II / inside bending radius, tube inside, etched with 1% HNO₃, 500:1

Fig. 9. The microstructure formation – inside and outside of the tube (cross section III) [11, 12, 13]:
a) radius III / inside bending radius, tube outside, etched with 1% HNO₃, 500:1,
b) radius III / inside bending radius, tube intside, etched with 1% HNO₃, 500:1

Figures 2 and 10 show a hot bent, highly stressed stabilizer bar. The applied 34MnB5 steel is an alloy steel with low carbon content. Despite the very short time of the bending process, the formation of proeutectoid ferrite occurs. Fig. 11 shows an isothermal transformation diagram for the 30MnB5 steel which has properties comparable to the 34MnB5 steel. The mechanism of ferrite formation in alloy steels with low carbon content (up to 0,45%) is shown in Fig. 12. The desired martensite transformation with bypassing the pearlite and bainite transformation areas does not occur here. The steel reaches a lower hardness (yellow line) about 318 HV (R_m = 1022 MPa)
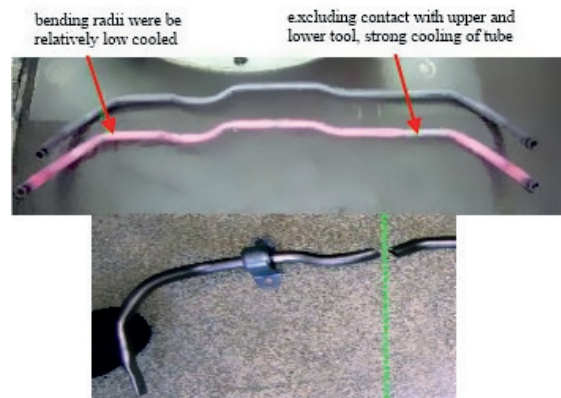

Fig. 10. Area of breakage – warm bending of tubular stabilizer bar in the bending table [12, 13]
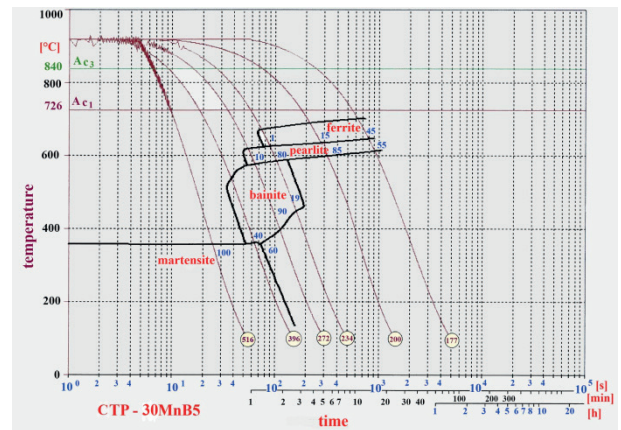

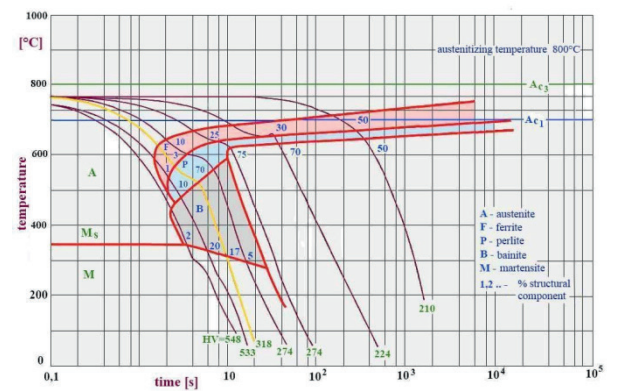Fig. 11. TTT diagram (time temperature trans formation) for steel 30MnB5 [14]

Fig. 12. TTT diagram (time temperature trans formation) for alloy steels with carbon content below 0,45% [15]

4. Discussion

The breaking point is not located where the greatest equivalent stresses occur (Fig 13 c, d). The stabilizer bar breaks there where the greatest proeutectoid ferrite precipitations occur (Fig. 2, bending radius I and Fig. 13b). The maximum equivalent stress at the breaking point is about 714,05 MPa. So the combination: high stresses connected with the ferrite precipitations resulted in the early destruction of the stabilizer bars. For tube stabilizer bars, hot bent with mechanically high stress, steel 34MnB5 is not recommended. The reason is ferrite formed in the radial zones and will lead to a fatigue fracture. In the case of stabilizer bars with mechanically low stress, formation of ferrite in the radial zones will be omitted.

It is reasonable to conduct more investigation for such important element in car vehicle. Taking into consideration all processes, starting from manufacturing [16-20], regular exploitation [21-24] and repairs [25-32].

Nowadays many of monitoring system allow observing of functionality and parameters of different elements [33-40].

5. Conclusion

In the process of tube bending the outer curve of the tube is elongated and the inner curve is upset forged. Furthermore, circumferential stress occurs. The consequences of this complex triaxial stress and deformation condition are displacements of the non–stretched layer towards the bending center, in circumferential direction – elongations of the stretched side and upsetting of the compression side, changes in the cross–sectional shape (ovalization) and an irregular distribution of cold work hardening over the cross–section and unrolling the bend in relation to longitudinal axis.

It is important that the intended weight reduction is not greater than 40 to 45 % of the weight of a comparable solid stabilizer bar. Weight savings exceeding beyond that lead to no longer acceptable wall thicknesses, thus to further loads which are caused by the warps of the tube. Such arch stresses have an extremely negative impact on the lifespan of the element. The outer and inner diameters can be calculated by the following equations [1–6]:

$$d_{i,tube} = d_{solid} \sqrt{\frac{1 - k^2}{2k}} \tag{1}$$

$$d_{a,tube} = d_{solid} \sqrt{\frac{1 + k^2}{2k}} \tag{2}$$

where:

$d_{i,a,tube}$ – inner or outer diameter of tube
d_{solid} – diameter of solid stabilizer bar
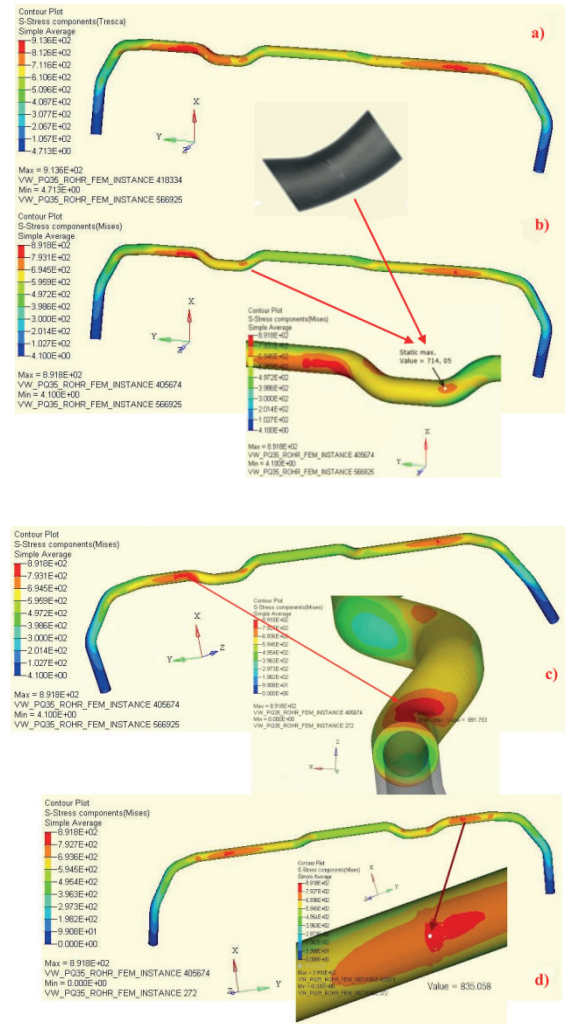k – weight fraction of the tube e.g. $k = 0,6$

Fig. 13. Finite Element Method (FEM) computations – central bending radii, bearing area (Fig. 2):
a) equivalent stresses according to Tresca (913,6 MPa),
b) equivalent stresses according to v. Mieses (714,05 MPa) – breakage / bending radius,
c) and d) equivalent stresses according to v. Mieses (891,8 MPa) – bending radius II,
d) equivalent stresses according to v. Mieses (835,1 MPa) – bearing area

A proper construction and the selection of parameters influence the strength properties, the weight, durability and reliability as well as the selection of an appropriate production method. The selection of the manufacturing process has a fundamental impact on the quality and durability of the stabilizer bars.
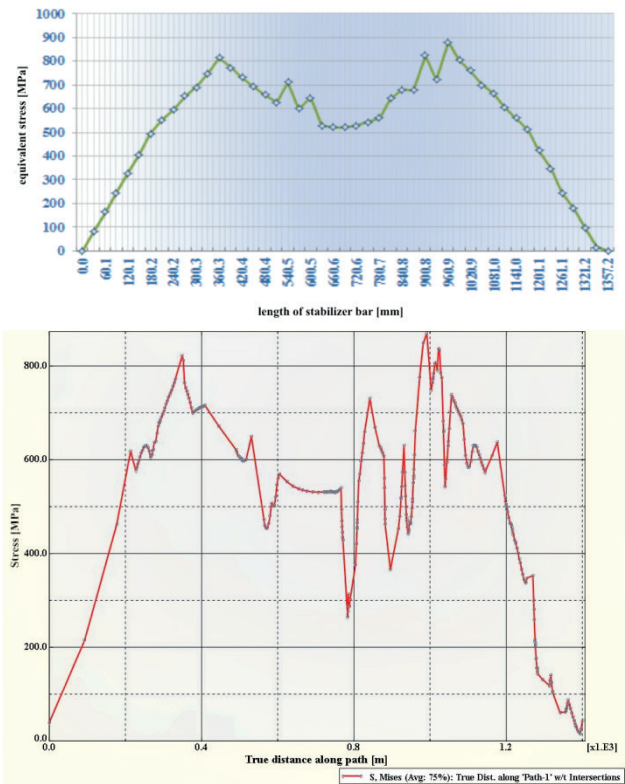
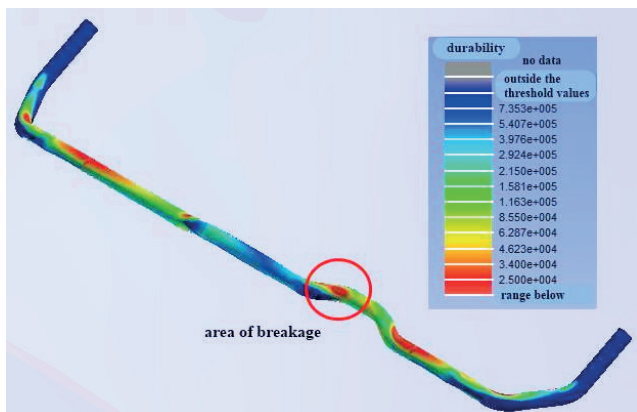Fig. 14. Equivalent stresses: a) analytical calculations, b) tension curve created with HyperWorks (FEM)

Fig. 15. Durability analysis – created with HBM nCode DesignLife

REFERENCES

[1] H. – E. v Estorff, Technische Daten Fahrzeugfedern Teil: 3 Stabilisatoren, Stahlwerke Brüninghaus GmbH, Werk Werdohl, Hang Druck KG, 97–113 Köln (1969).

[2] J. Ulbricht, H. Vondracek, Warm geformte Federn – Leitfaden für Konstruktion und Fertigung, Hoesch Werke, Hohenlimburg Schwerte AG, W. Stumpf KG, 1–36, 139–150 Bochum (1973)

[3] F. Fischer, H. Vondracek, Warm geformte Federn – Konstruktion und Fertigung, Hoesch Werke, Hoesch Hohenlimburg AG, W. Stumpf KG, 161–171, 177–193 Bochum (1987)

[4] P. Gebauer: Stabilisatoren für Kraftfahrzeuge, ThyssenKrupp Bilstein Suspension GmbH, 1–29 Esslingen (2007)

[5] H. Dziemballa, L. Manke, Gewichtsredu–zierung durch hochbeanspruchte Rohrstabili–satoren, ThyssenKrupp Technoforum 2004, 28–33 Essen (2004)

[6] B. Heißing, M. Ersoy, Fahrwerkhandbuch – Grundlagen, Fahrdynamik, Komponenten, Systeme, Mechatronik, Perspektiven. 2. Auflage, Vieweg + Teubner, 77–78, 231–239 Wiesbaden (2008)

[7] B. Klein, FEM – Grundlagen und Anwendungen der Finite – Element – Methode im Maschinen– und Fahrzeugbau, 7. Auflage, Vieweg Studium Technik, 34 – 88, 323 – 356 Wiesbaden (2007)

[8] Schulungsunterlagen HyperWorks11, Radioss, Manufacturing Solutions 11.0 HyperForm Tutorial, Fa. Altair Deutschland GmbH, Hannover (2012)

[9] A.M. Wittek, Wpływ czynników konstrukcyjnych i technologicznych na trwałość stabilizatorów w pojazdach samochodowych, Ph.D dissertation, 44 – 60, 99 – 113, 187 – 205 Katowice (2013)

[10] DIN EN ISO 3887: Steels – Determination of depth of decarburization (ISO 3887:2003), German version of EN ISO 3887, 1–9 (2003)

[11] Prüfbericht – Nr.: 1068(09 – LVQ – WP GmbH, 1–9 (05.10.2009)

[12] Prüfbericht – Nr.: 095018591 – Hoesch Hohenlimburg GmbH, 1–8 (23.09.2009)

[13] Prüfbericht, Projekt: Warmbiegen von Rohren V6, Versuchsdaten– und Ziele, ThyssenKrupp Bilstein Suspension GmbH, 1–16 (07.10.2009)

[14] Salzgitter Flachstahl GmbH, Eisenhüttenstraße 99, 38239 Salzgitter: Technische Datenblätter, http://www.salzgitterflachstahl.de/de/Produkte/warmgewalzte_produkte/stahlsorten/borlegierte_Verguetungsstaehle/, 1–2 (28.12.2013)

[15] W. Weißbach, Werkstoffkunde. Strukturen, Eigenschaften, Prüfung. 16. Auflage, Friedriech Vieweg & Sohn Verlag, 161 – 169 Wiesbaden (2007)

[16] L. Blacha, R. Burdzik, A. Smalcerz, T. Matuła, Effects of pressure on the kinetics of manganese evaporation from the OT4 alloy, Archives Of Metallurgy And Materials **58** (1), 197-201 (2013).

[17] A. Kaźmierczak-Bałata, J. Bodzenta, D. Trefon-Radziejewska, Determination of thermal-diffusivity dependence on temperature of transparent samples by thermal wave method, International Journal of Thermophysics **31** (1), 180-186 (2010).

[18] L. Blacha, R. Burdzik, A. Smalcerz, T. Matuła, Effects of pressure on the kinetics of manganese evaporation from the OT4 alloy, Archives Of Metallurgy And Materials **58** (1), 197-201 (2013).

[19] L. Blacha, G. Siwiec, B .Oleksiak, Loss of aluminium during the process of Ti-Al-V alloy smelting in a vacuum induction melting (VIM) furnace, Metalurgija **52** (3) 301-304 (2013).

[20] G. Siwiec, B .Oleksiak, A. Smalcerz, J. Wieczorek. Surface tension of Cu-Ag alloys, Archives of Materials and Metallurgy **58** (1), 193-195 (2013).

[21] R. Burdzik, Ł. Konieczny, Research on structure, propagation and exposure to general vibration in passenger car for different damping parameters, Journal of Vibroengineering **15**(4), 1680-1688 (2013).

[22] R. Burdzik, Research on the influence of engine rotational speed to the vibration penetration into the driver via feet - multidimensional analysis, Journal of Vibroengineering **15**(4), 2114-2123 (2013).

[23] R. Burdzik, Identification of structure and directional

distribution of vibration transferred to car-body from road roughness, submitted to Journal of Vibroengineering **16**(1), 324-333(2014).

[24] R. Burdzik, Implementation of multidimensional identification of signal characteristics in the analysis of vibration properties of an automotive vehicle's floor panel, Eksploatacja i Niezawodnosc – Maintenance and Reliability 16(3), 439-445 (2014).

[25] J. Slania,, Influence of phase transformations in the temperature ranges of 1250-1000ºC and 650-350ºC on the ferrite content in austenitic welds made with T 23 12 LRM3 tubular electrode. Archives of Metallurgy and Materials, 3 (2005).

[26] J. Slania, B. Slazak, M. Fidali, Application of fast fourier transform (FFT) in the analysis of a welding current instantaneous values waveforms during welding with a covered electrode, Arch. Metall. Mater. **59**(2), 569-573 (2014).

[27] G. Golański, J. Słania, Effect of different heat treatments on microstructure and mechanical properties of the martensitic GX12CrMoVNbN91 cast steel. Archives of Metallurgy and Materials, **4** (2012).

[28] T. Węgrzyn, The Classification of metal weld deposits in terms of the amount of nitrogen, Proceedings . Conference of International Society of Offshore and Polar Engineers ISOPE´2001, Stavanger, Norway 2001, International Society of Offshore and Polar Engineers, vol. IV, Cupertino – California, USA, 2001 282-285.

[29] T. Węgrzyn Mathematical Equations of the Influence of Molybdenum and Nitrogen in Welds. Conference of International Society of Offshore and Polar Engineers ISOPE´2002, Kita Kyushu, Japan 2002, Copyright by International Society of Offshore and Polar Engineers, vol. IV, ISBN 1-880653-58-3, Cupertino – California – USA 2002.

[30] T. Węgrzyn, J. Piwnik, B. Łazarz, D. Hadryś, Main micro-jet cooling gases for steel welding. Archives of Materials and Metallurgy **58**(2), 551-553 (2013).

[31] A. Lisiecki, Diode laser welding of high yield steel. Proceedings of SPIE, Laser Technology, Applications of Lasers 8703, 22 (2012).

[32] A. Lisiecki, Welding of titanium alloy by Disk laser. Proceedings of SPIE, Laser Technology, Applications of Lasers, 87030 (2013).

[33] P. Łubkowski, D. Laskowski, Communication in Computer and Information Science **71**, 59 (2015).

[34] J. Pankiewicz, P. Deuszkiewicz, J. Dziurdź, M. Zawisza, Advanced Mater. Res. **1036**, 586 (2014).

[35] R. Doleček, O. Černý, P. Sýkora, J. Pidanič, Z. Němec, International Conference on Power Engineering, Energy and Electrical Drives, IEEE CFP1397B-POD, Turkey, 650 (2013).

[36] M. Kozłowski, W. Choromański, J. Kowara, Journal of Vibroengineering **17**(3), 1436 (2015).

[37] G. Grzeczka, K. Listewnik, M. Kłaczyński, W. Cioch, Journal of Vibroengineering **17**, 4025 (2015).

[38] A.N. Wieczorek, Archives of Metallurgy and Materials **59**(4), 1665 (2014).

[39] A.N. Wieczorek, Archives of Metallurgy and Materials **59**(4), 1675 (2014).

[40] T. Wegrzyn, J. Piwnik, B. Łazarz, W. Tarasiuk, Mechanics 21(5), 419 (2015).